ACS Photonics

Article

pubs.acs.org/journal/apchd5

Giant Enhancement of Upconversion Fluorescence of $NaYF_4$:Yb^{3+},Tm^{3+} Nanocrystals with Resonant Waveguide Grating Substrate

Jian Hung Lin,[†] Hao Yu Liou,[†] Chen-Dao Wang,[‡] Chun-Yen Tseng,[§] Ching-Ting Lee,[§] Chu-Chi Ting,[‡] Hung-Chih Kan,*[,†] and Chia Chen Hsu*[,†,‡]

[†]Department of Physics and [‡]Graduate Institute of Opto-Mechatronics, National Chung Cheng University, Ming Hsiung, Chia Yi 621, Taiwan

[§]Institute of Microelectronics, Department of Electrical Engineering, National Cheng Kung University, Tainan 701, Taiwan

Supporting Information

ABSTRACT: By embedding $NaYF_4$:Yb^{3+},Tm^{3+} nanocrystals into the top cladding layer of a resonant waveguide grating structure, we demonstrate that the upconversion fluorescence of Tm^{3+} ions can be greatly enhanced, by a factor of up to 10^4. The resonant waveguide grating structure consists of an SU8 bottom layer with sinusoidal grating morphology coated with a thin TiO_2 waveguide layer and then covered with a poly(methyl methacrylate) cladding layer doped with $NaYF_4$:Yb^{3+},Tm^{3+} nanocrystals. The giant enhancement of the upconversion fluorescence is achieved first by coupling the excitation light with a guided mode of the resonant waveguide grating structure and then the fluorescent light with a second guided mode. Our numerical simulation results obtained by rigorous coupled-wave analysis indicate that the electric field of the incident light is strongly enhanced near the interface of the TiO_2 layer and the poly(methyl methacrylate) layer at guided mode resonance, and this is the major effect of the observed enhancement of the upconversion fluorescence of the nanocrystals. The resonance between the fluorescent emission and the waveguide structure further enhances the intensities of the fluorescent signal. We also find that the lifetime of upconversion fluorescence at 480 nm wavelength from the rare-earth nanocrystals is reduced about 1.34-fold when both excitation and extraction resonance occurs in the waveguide structure.

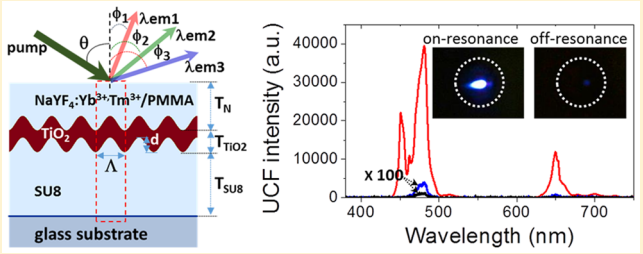

KEYWORDS: *upconversion, rare-earth nanocrystals, resonant waveguide grating, guided mode resonance, excitation resonance, extraction resonance*

Rare-earth (RE) doped upconversion (UC) nanocrystals[1−3] have attracted great interest due to their potential applications in photonic and biomedical systems.[4−10] Highly efficient UC nanocrystals are typically composed of a sodium yttrium fluoride ($NaYF_4$) lattice codoped with lanthanide ions, including ytterbium (Yb^{3+}) sensitizer ions and activator ions such as erbium (Er^{3+}), thulium (Tm^{3+}), or holmium (Ho^{3+}).[11,12] The sensitizer Yb^{3+} ions absorb near-infrared (near-IR) radiation and then transfer their photon energy to activator ions multiple times, which results in multiphoton transition process.[12] Therefore, the excited activator ions emit photons in several distinct and narrow emission bands over ultraviolet, visible, and near-IR wavelengths. Compared with the efficiencies of other UC mechanisms such as two-photon fluorescence (TPF), sum frequency generation, or nonlinear harmonic generation, the UC fluorescence (UCF) efficiency generated by RE-doped UC nanocrstals is much higher due to real-state energy transitions involved in the multiphoton transition process.[12] However, to date the UCF efficiency of RE-doped UC nanocrytals is still quite low. Although various methods have been proposed to enhance the UCF efficiency, the highest enhancement factor that has been achieved is still too low for practical applications.[13−15] Therefore, it is important to develop a technique that can greatly improve the UCF efficiency of RE-doped UC nanocrytals and make the UCF of RE-doped UC nanocrystals suitable for innovative biosensing, bioimaging, solid-state lasers, and solar cell applications.

All-dielectric and low-loss resonant waveguide grating (RWG)[16−19] structures are widely used to enhance light and matter interactions such as photoluminescence of fluorescent dyes and quantum dots[17,19,20] and nonlinear optical (NLO) harmonic generation.[21−23] An RWG typically consists of a high-refractive-index grating-waveguide layer and a low-refractive-index supporting layer, and it can produce very sharp reflection and transmission anomalies that characterize the guided mode resonance (GMR).[19] Strong light−matter interaction can be achieved by matching either incoming excitation or outgoing emission wavelength with the guided mode wavelengths of the RWG.[19,20] Indeed, when the incoming excitation wavelength matches the GMR wavelength, which we refer to as "resonant

Received: November 13, 2014
Published: March 23, 2015

ACS Publications © 2015 American Chemical Society

DOI: 10.1021/ph500427k
ACS Photonics 2015, 2, 530−536

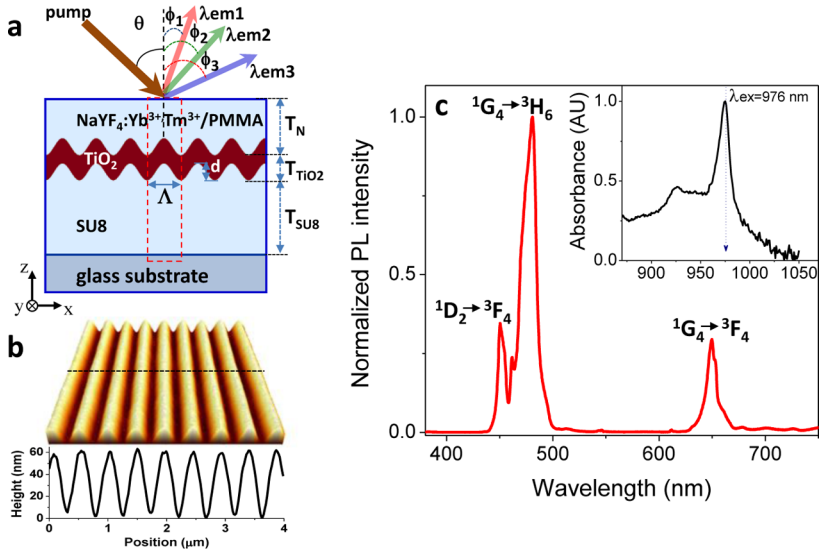

Figure 1. (a) Schematic of the 1D RE-doped polymer RWG. Angles θ and ϕ_i's are the incident excitation angle and the UCF detection angles relative to the surface normal direction, respectively. The dashed rectangle (red color) defines the unit cell used for simulations. (b) AFM image of the TiO_2 RWG. The spatial period (Λ) and the groove depth (d) of the grating are 466 and 60 ± 5 nm, respectively. (c) UCF spectrum of a $NaYF_4$:Yb^{3+},Tm^{3+}/PMMA thin film. Inset shows the absorption spectrum of $NaYF_4$:Yb^{3+},Tm^{3+} nanocrystals dissolved in toluene solution.

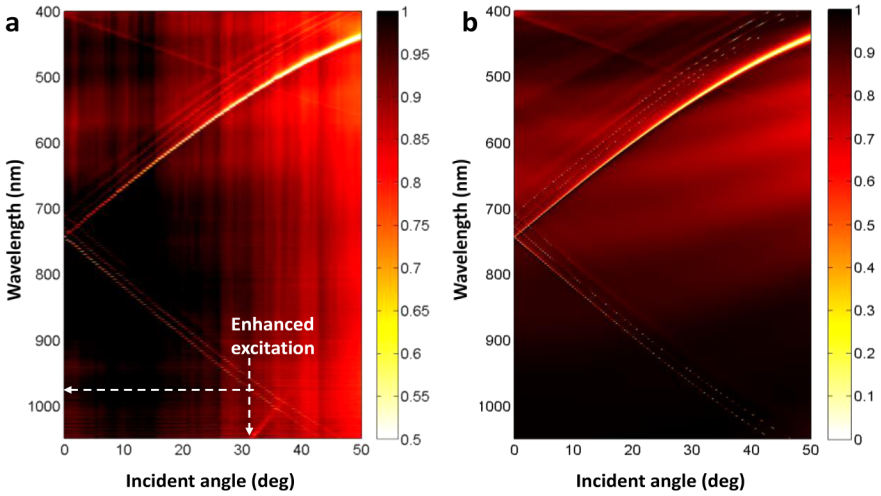

Figure 2. (a) Measured transmittance in TE mode of the RE-doped polymer RWG as a function of incident angle and wavelength. The horizontal and vertical dashed lines highlight the GMR mode at 976 nm with incident angle $\theta \approx 31.5°$. (b) Transmittance of the RE-doped polymer RWG calculated with the RCWA method. The parameters used in the calculation are Λ = 466 nm, T_N = 200 nm, T_{TiO2} = 55 nm, and T_{SU8} = 1500 nm. The dispersion properties of the refractive indices of TiO_2, $NaYF_4$:Yb^{3+},Tm^{3+}/PMMA, SU8, and glass were used in the calculation.

excitation", a strong local field is formed at the grating surface. Therefore, the fluorescence or NLO harmonic signal can be dramatically enhanced if fluorescent or NLO molecules are in direct contact with the grating. Additionally, as the outgoing wavelengths of the fluorescence or NLO harmonic signal overlap with the GMR wavelength, which we refer to as "resonant extraction", the extraction of fluorescence or NLO harmonic signal can be further increased due to the high reflection efficiency associated with the GMR. This indeed has been reported for the case of one-photon fluorescence (OPF) and TPF.[19,24]

RESULTS AND DISCUSSION

In this paper we report on an RWG structure that fulfills both resonance conditions described above and indeed produces tremendous enhancement of UCF from RE-doped UC nanocrystals. A thin layer of polymer doped with RE UC nanocrystals was deposited on top of the waveguide layer of an all-dielectric RWG. The RWG is a one-dimensional sinusoidal grating structure whose period was designed based on results of the rigorous coupled-wave analysis (RCWA)[25] such that the RWG with the polymer top layer supports GMRs at the excitation and emission wavelengths of the UC process. A two-beam interference technique[26,27] combined with the electron-beam deposition method was used to fabricate the sinusoidal RWG structure, which consists of an SU8 substrate and a thin TiO_2 waveguide layer. We demonstrate the UCF signal generated from the RE-doped polymer thin layer coated on top of such an RWG structure can be enhanced up to 10^4 times when both excitation and extraction resonance are simultaneously achieved.

Details of the design of the 1D RE-doped polymer RWG are shown in Figure 1a. The structure consists of, from top to bottom, a $NaYF_4$:Yb^{3+},Tm^{3+} nanocrystals doped poly(methyl

DOI: 10.1021/ph500427k
ACS Photonics 2015, 2, 530−536

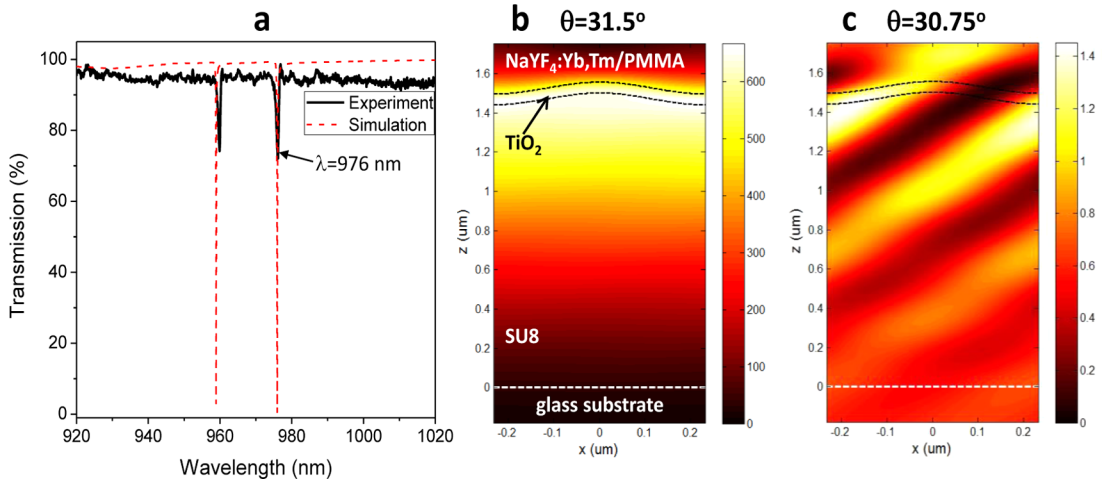

Figure 3. (a) Measured (solid curve) and calculated (dashed curve) transmission spectra of the RE-doped polymer RWG for the TE mode polarization at the incident angle of 31.5°. Calculated electric-field intensity ($|E^2|$) distribution of the TE GMR mode for λ = 976 nm at (b) θ = 31.5° (on-resonance) and (c) θ = 30.75° (off-resonance).

methacrylate) ($NaYF_4$:Yb^{3+},Tm^{3+}/PMMA) thin layer, a 1D sinusoidal waveguide grating (TiO_2), a bottom cladding layer (SU8), and a glass substrate. In order to have transverse-electric (TE) GMR modes at excitation and emission wavelengths, the TiO_2 layer was designed to be 60 nm thick (T_{TiO2}) with a periodicity of 466 nm. From SEM measurement, the thickness of SU8 (T_{SU8}), TiO_2 (T_{TiO2}), and $NaYF_4$:Yb^{3+},Tm^{3+}/PMMA (T_N) thin layers was determined to be 1400 ± 100, 60 ± 5, and 250 ± 20 nm, respectively (see Supporting Information, Figure S1). Figure 1b shows the atomic force microscope (AFM) image of the fabricated TiO_2 RWG structure. The total area of the RWG is 6 × 6 mm^2 on the sample. From the AFM measurement, the period Λ and depth d of the grating were determined to be 466 and 60 ± 5 nm, respectively. For RCWA simulations, the refractive indices of $NaYF_4$:Yb^{3+},Tm^{3+}/PMMA (n_N), SU8 (n_{SU8}), and TiO_2 (n_{TiO2}) were determined by ellipsometry measurements, and the refractive index of the glass substrate was adopted from ref 28.

Figure 1c plots the UCF spectrum of a $NaYF_4$:Yb^{3+},Tm^{3+}/PMMA thin film excited by a 976 nm wavelength laser beam with an intensity of 200 W/cm^2. There are three dominant emission bands centered around 450, 480, and 650 nm, corresponding to $^1D_2 \rightarrow {}^3F_4$, $^1G_4 \rightarrow {}^3H_6$, and $^1G_4 \rightarrow {}^3F_4$ transitions of Tm^{3+} ions, respectively.[29] The inset of Figure 1c shows the absorption spectrum of $NaYF_4$:Yb^{3+},Tm^{3+} nanocrystals dissolved in a toluene solution. The absorption of the nanocrystals peaks at 976 nm wavelength.

Figure 2a shows the measured and simulated transmittance of the GMR modes in the RE-doped polymer RWG as a function of incident angle and wavelength for TE polarization incidence. Related angular-resolved transmission spectral data can be found in the Supporting Information, Figure S2. At each incident angle the transmission minima characterize the GMR mode of the RWG. The measurement is in good agreement with the simulation, except that transmittance at the GMR in the experiment is higher than that in the simulation. This is probably due to the difference between the real grating structure and the ideal sinusoidal grating assumed in the simulation. The GMR mode at normal incidence occurs at 743 nm wavelength in the measurement. As the incident angle increases, the GMR mode splits into two separate modes due to the first-order diffraction from the grating;[24] one red-shifts with the incident angle, and the other blue-shifts. The red-shifted GMR mode was used for resonant excitation, which occurs at λ = 976 nm and θ = 31.5°. Blue-shifted GMR modes were used for resonant extraction, which occurs at the following angles: ϕ = 46°, 39° and ϕ = 14° for emission at 450, 480, and 650 nm wavelengths, respectively.

The effect of the resonant excitation on the UCF of the RE-doped polymer RWG was first investigated. Figure 3a shows the measured and calculated transmission spectra of the RE-doped polymer RWG for the TE mode at θ = 31.5°. There are GMR modes at 960 and 976 nm. Figure 3b shows the calculated electric-field intensity ($|E^2|$) distribution in the RE-doped polymer RWG for the TE GMR mode with λ = 976 nm at θ = 31.5° (on-resonance). The electric field is highly concentrated in the TiO_2 layer. This indicates that for the GMR mode at angle θ = 31.5° the incident light intensity is mainly localized in the TiO_2 layer. The strong localized electric field located at the interface between the $NaYF_4$:Yb^{3+},Tm^{3+}/PMMA, TiO_2, and SU8 layers is very crucial for the UCF output. Nearly 600-fold enhancement is predicted for the "local field" at the interface of the TiO_2 grating. In contrast, Figure 3c shows that for the case of slightly off-resonance (θ = 30.75°) at the same wavelength minimal electric-field intensity enhancement is predicted at the interfaces of the TiO_2 grating and neighboring layers. In fact, the GMR mode at λ = 960 nm shown in Figure 3a can also be shifted to 976 nm spectrally by increasing the incident angle to 34° according to Figure 2a. However, since this resonant mode provides a smaller UCF enhancement compared to the GMR mode at longer wavelength, we thus focus on the GMR mode at longer wavelength for the discussion below.

For the fluorescence measurement, a collimated 976 nm wavelength laser beam (beam diameter = 0.76 mm) with a power of 300 mW was used to excite the sample with the GMR mode at 976 nm wavelength shown in Figure 3a, and the detection angle ϕ was set to 0°. The incident angle θ was scanned from 0° to 35° in steps of 0.25°. Figure 4a displays the UCF spectra obtained with the sample illuminated at the resonant angle θ = 31.5° and the nonresonant angle θ = 30.75°. The UCF spectrum obtained with θ = 31.5° shows remarkably high intensities with narrow bands centered at 450, 480, and 650 nm wavelengths. With a very small change in the incident angle, i.e., from 31.5° to 30.75°, the intensity of UCF decreases dramatically, and it becomes comparable to that measured from a nonpatterned area on the

DOI: 10.1021/ph500427k
ACS Photonics 2015, 2, 530−536

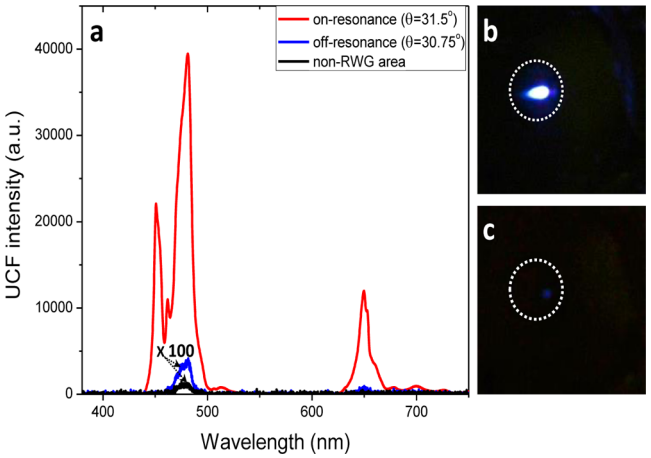

Figure 4. (a) UCF spectra of the RE-doped polymer RWG under on-resonance (θ = 31.5°) and off-resonance (θ = 30.75°) and that from a nonpatterned area (labeled as "non-RWG area"). Panels (b) and (c) are optical images of UCF of the sample when illuminating the excitation beam under (b) on-resonance (θ = 31.5°) and (c) off-resonance (θ = 30.75°) conditions, respectively.

sample. Figure 4b and c show the optical images of the fluorescent emission of the sample taken at the resonant excitation (θ = 31.5°) and nonresonant excitation (θ = 30.75°). The circular region on each image indicates the lateral range of the RWG structure. The UCF emission is quite bright at resonant excitation and barely visible at the nonresonant condition. The giant enhancement of the UCF obtained at resonant angle excitation (θ = 31.5°) clearly agrees with the simulated enhancement of the electric field of the excitation light at the interface between the TiO_2 waveguide layer and the $NaYF_4$:Yb^{3+},Tm^{3+}/PMMA layer at excitation resonance conditions.

Next we investigated the effect of enhanced extraction by matching a GRM mode to the wavelengths of the UCF emission, which has been reported to produce further enhancement of the OPF[20] or TPF[24] signal with the RWG. In the experiment, the sample was illuminated under resonant-excitation condition (θ = 31.5°), and the detection angle was varied from 0° to 50° in steps of one degree. Figure 5a shows the logarithmic plot of UCF intensities as a function of wavelength and detection angle, and the dashed line reproduces the spectral positions of the GMR mode as a function of the incident angle shown in Figure 2a. It is clear that each UCF band yields maximum emission intensity when its center wavelength coincides with the GMR wavelength, i.e., the condition for resonant extraction. This is shown quantitatively in Figure 5b: the UCF spectrum obtained at ϕ = 0°, which corresponds to conditions of no extraction enhancement, and the UCF spectra obtained at ϕ = 14° , 39°, and 46°, which correspond to conditions of resonant extraction for emission bands centered at 650, 480, and 450 nm wavelengths, respectively. It is clear that for the same emission band the highest emission peak intensities occur at resonant-extraction conditions. Comparing the UCF intensities obtained from resonant and nonresonant extraction, the UCF emission is further enhanced about 3 times. This improvement is similar to those observed in previous OPF[20] and TPF[24] experiments.

To characterize the UC mechanisms of the enhanced fluorescence observed from our samples, we investigated the excitation intensity dependence of the UCF intensities. Figure 6a displays the logarithmic plot of the UCF intensities versus the excitation intensity obtained from the RE-doped polymer RWG sample under the condition of excitation resonance. Figure 6b is from the same sample but with both excitation and extraction resonance conditions achieved, and Figure 6c is from a nonpatterned area. For the case of the nonpatterned area, the UCF intensity excited with a collimated beam was too weak to be detected; we thus employed a convex lens with a focus length of 20 cm to focus the excitation beam into a spot of 0.37 mm diameter on the sample to increase the UCF intensity. In the low excitation intensity limit, the emission intensity is predicted to be proportional to the nth power of the excitation intensity, where n corresponds to the number of photons required to populate the excited state responsible for the emitted photon.[30,31] In Figure 6a the power exponents n are determined to be 4.6, 3.1, and 3.2 for the emission peaks centered at 450, 480, and 650 nm,

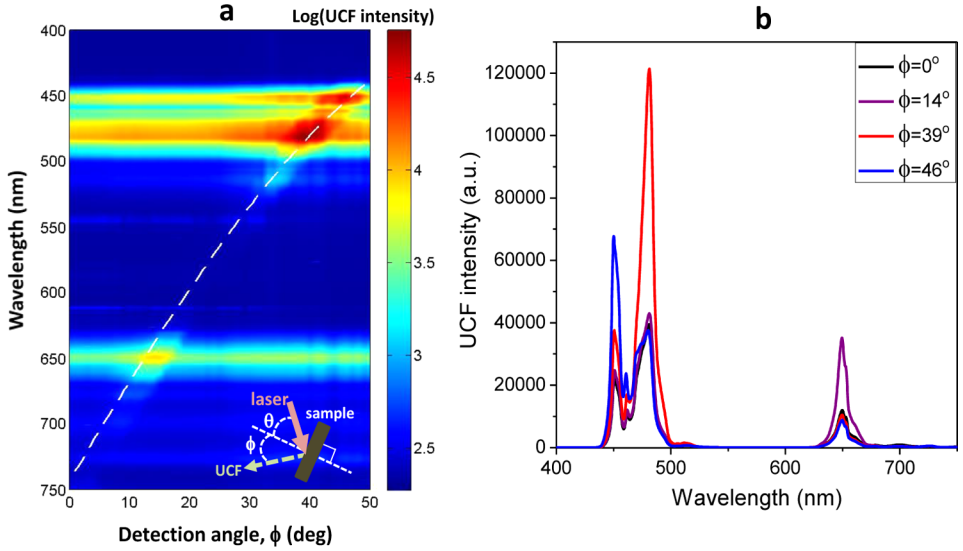

Figure 5. (a) Logarithmic plot of the UCF spectra of the RE-doped polymer RWG as a function of the detection angle (ϕ) under excitation resonance (θ = 31.5°). White dashed line displays the peak wavelength of the GMR versus the launched angle. Inset shows the configuration of the UCF measurement. (b) Comparison of the UCF spectra under excitation resonance with four detection angles: ϕ = 0°, 14°, 39°, and 46°.

DOI: 10.1021/ph500427k
ACS Photonics 2015, 2, 530−536

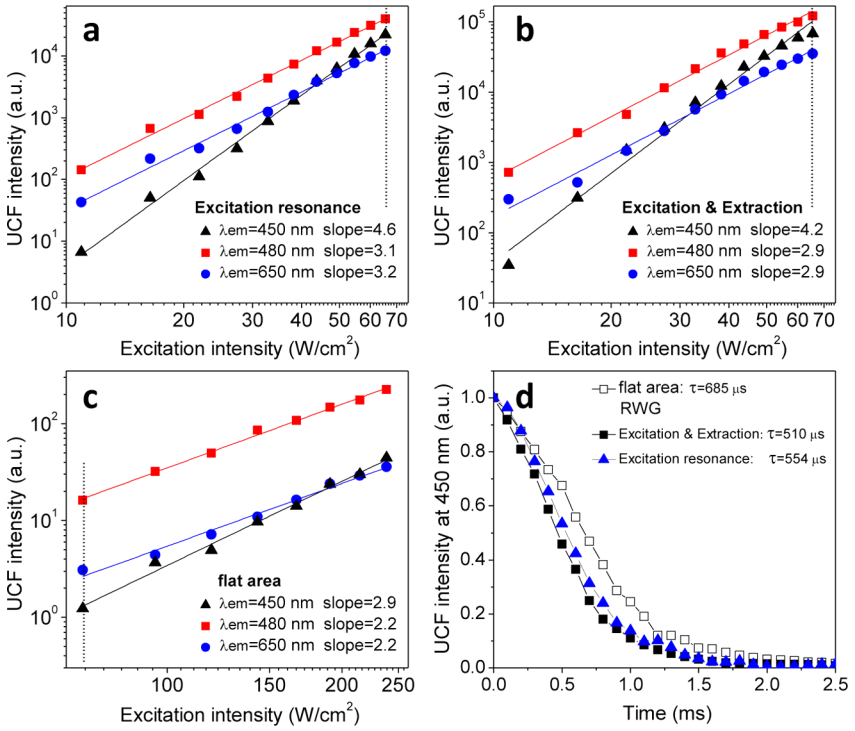

Figure 6. Excitation dependences of various UCF peak intensities obtained from the RE-doped polymer RWG under (a) excitation resonance and (b) simultaneous excitation and extraction resonance, and (c) the UCF from a nonpatterned area. (d) Decay of the UCF emission at λ_e = 480 nm obtained from the non-RWG area and RWG area when excitation resonance only, or simultaneous excitation and extraction resonance, is achieved.

respectively, and in Figure 6b the corresponding exponents are 4.2, 2.9, and 2.9. These values are consistent with the proposed four-photon and three-photon processes for populating Tm^{3+} ions in the $^1D_2$ state and the $^1G_4$ state, respectively.[32−34] For the nonpatterned area, Figure 6c shows that the power exponents of the excitation intensity dependence in the range 70−250 W/cm^2 are 2.9, 2.2, and 2.2 for emission peaks centered at 450, 480, and 650 nm, respectively, which are smaller by 1 order of magnitude compared to the corresponding power exponents in Figure 6a and b. Similar results have been reported previously,[35,36] and indeed reduction in the value of the power exponent has also been predicted for the case of a high excitation intensity limit.[30,31] Although the excitation intensity is nominally higher for the case of a nonpatterned sample, the results of simulations shown in Figure 3b indicate that the enhancement of the E-field near the PMMA/TiO_2 interface of the RWG sample effectively enhances the excitation intensity by 1 order of magnitude. Therefore, the excitation intensities are roughly the same in both RWG and nonpatterned samples. This implies that the power exponents should be similar in both cases. A plausible explanation for why the RWG sample has higher power exponents that resemble those of the low excitation intensity limit follows. In the simple models proposed by Pollnau et al.[30] and by Suyver et al.,[31] the sense of "high" or "low" for the excitation intensities depends on the relative magnitude of the excitation rate of Tm^{3+} ions and the rates at which the excited Tm^{3+} ions decay. For a given excitation intensity, a high decay rate of excited Tm^{3+} ions gives a power exponent for the case of a "low" excitation limit, and vice versa. In our case, it is the enhancement of the decay rates of excited Tm^{3+} ions that makes the RWG sample demonstrate "low" excitation intensity dependence of the UCF intensities. This is supported by our measurement of the UCF emission lifetime for the case of 480 nm UCF emission. Figure 6d shows the decay of the UCF emission obtained from the RE-doped polymer RWG and that from the nonpatterned area with the excitation intensity of 65 W/cm^2. A chopper was used to modulate the excitation beam, and a photomultiplier (PMT) detector was used to detect the UCF emission at 480 nm. An interference filter at 480 nm and an IR filter were placed in front of the PMT to ensure only the desired UCF emission is detected. The results indicate that the lifetime of the excited Tm^{3+} ions (in the $^1G_4$ state) in the RWG is 510 μs, in contrast to the 685 μs lifetime of those in the nonpatterned area. Therefore, the decay rate of the Tm^{3+} ions is indeed enhanced for the case of the RWG sample, thus shifting the excitation intensity dependence of the UCF emission toward the low-intensity limit.

Previous papers reported that the increase of radiative relaxation rate occurs in a plasmon-enhanced UC system when the emission wavelength of RE ions matches the wavelengths in the surface plasmon resonance band.[13−15] The metal nanostructures produce an environment with higher local photon density states at the emission wavelength of RE ions, which facilitates the relaxation of excited RE ions and results in a shorter UCF lifetime. Just like the plasmon-enhanced UC system, we did expect to observe the increase of the radiative relaxation rate of Tm^{3+} ions in the RWG sample for the case of simultaneous excitation and extraction resonance. However, as shown in Figure 6d, the lifetimes of the Tm^{3+} ions in the RWG sample for both simultaneous excitation and extraction resonance and excitation resonance only cases are of similar magnitude, which is beyond our expectation. The result suggests that the RWG alone is sufficient in enhancing the decay rate of the Tm^{3+} ions, possible due to modification of local photon density of states of the emitted photons by boundary conditions set by the RWG structure.

Finally, to quantify the UCF enhancement factors, the UCF intensities obtained at the excitation intensity around 65 W/cm^2 (marked by the vertical dotted lines in Figure 6a−c in each case)

DOI: 10.1021/ph500427k
ACS Photonics 2015, 2, 530−536

were chosen to determine the UCF enhancement factors, which is defined as the ratio of the UCF intensity generated from the RWG to that of the nonpatterned area. Table I summarizes the

Table I. Summary of Enhancement Factors of Three Emission Wavelengths at 450, 480, and 650 nm of the RE-Doped Polymer RWG under Excitation Resonance and Simultaneous Excitation and Extraction Resonance

	enhancement factor		
	λ_e = 450 nm	λ_e = 480 nm	λ_e = 650 nm
excitation resonance	2.2×10^4	2.8×10^3	5.6×10^3
excitation and extraction resonance	6.8×10^4	8.8×10^3	1.6×10^4

UCF enhancement factors of the RE-doped polymer RWG at three emission wavelengths. For the case of excitation resonance, the enhancement factors for emission wavelengths at 450, 480, and 650 nm are 2.2×10^4, 2.8×10^3, and 5.6×10^3, respectively, while for the case of simultaneous excitation and extraction resonance they are increased to 6.8×10^4, 8.8×10^3, and 1.6×10^4, respectively. The much larger UCF enhancement factors obtained in this work employed the same fundamental mechanism as the other GMR-enhanced light−matter interactions did, such as OPF, TPF, SHG, and THG.[17,19−23] The present RWG structure builds up a strongly enhanced local field around the UC nanocrystals and leads to highly efficient near-IR absorption at the excitation resonance condition. However, the power dependence of the UCF intensity on excitation flux associated with nonlinear four-photon or three-photon absorption transitions experienced by the Tm^{3+} ions is the major reason for achieving the record high enhancement factors in this work. Finally, the maintenance of the higher exponent power dependence relationship, resulting from the increase of the radiative relaxation rate of Tm^{3+} ions, also contributes to the high enhancement factors.

CONCLUSION

We have demonstrated that the UCF emission can be enhanced up to 10^4 times in the blue and red color regions by embedding an RE-doped polymer thin film on the top of a TiO_2 RWG and fulfilling the requirements of resonant excitation and resonant extraction conditions. The giant UCF enhancement is due to the strong local field built up near the TiO_2 grating and the $NaYF_4$:Yb^{3+},Tm^{3+}/PMMA thin layer interface when the excitation light at 976 nm resonates with the GMR. The extraction of the UCF emissions was promoted nearly 3-fold when the emission wavelengths aligned with their associated GMRs due to high reflectivity of the resonant mode. Compared with a non-RWG sample, a 1.34-fold reduction of the lifetime of the UCF at 480 nm in the RE-doped polymer RWG was found, when a simultaneous excitation and extraction resonance condition was met. Our results suggest that the giant enhancement of UCF achieved with a resonant waveguide grating substrate with a layer of lanthanide-doped nanocrystals on top makes UCF practical for biosensing and solar cell applications.

MATERIALS AND METHODS

Fabrication of the RE-Doped Polymer RWG Structure. A one-dimensional SU8 grating was first fabricated on top of a glass substrate by a two-beam interference technique,[26,27] and then a TiO_2 layer was deposited on top of the SU8 grating by the electron-beam deposition technique. The RE-doped polymer RWG was obtained by spin-coating of a $NaYF_4$:Yb^{3+},Tm^{3+}/PMMA solution on top of the TiO_2 layer and then baking for 1 h at 70 °C on a hot plate. The RE nanocrystalline phosphors ($NaYF_4$: 20 mol % Yb^{3+}, 2 mol % Tm^{3+}) were synthesized by adopting a thermal decomposition method.[37] The mean size of the $NaYF_4$:Yb^{3+},Tm^{3+} nanocrystals is 30 nm, determined by transmission electron microscopy measurement. A $NaYF_4$:Yb^{3+},Tm^{3+}/PMMA solution was prepared by doping $NaYF_4$:Yb^{3+},Tm^{3+} nanocrystals into PMMA with 20 wt % concentration in toluene.

UCF Measurement. In the experiment, a solid-state diode laser capable of outputting a CW laser beam at the wavelength of 976 nm with a power of 0.5 W was employed to excite the UCF sample. The laser beam was collimated into a 0.76 mm diameter beam, and its excitation power was adjusted with the combination of a half-wave plate and a polarizer. A grating spectrometer (Andor Shamrock SR-500i) adapted with a fiber head was used to collect and analyze UCF signals emitted from the sample. An IR filter was used to block the excitation beam from reaching the spectrometer. Figure 1a shows the orientations of the incident beam and the resonant fluorescent emission relative to the sample surface. The incident plane is the $x-z$ plane, the x-axis is the direction of the grating vector of the RE-doped polymer RWG sample, and z-axis is the direction normal to the top surface of the sample. The incident angle θ is measured with a precision of 0.5 degree. For the measurements of the dependence of the UCF on the emission angle ($\phi_{1,2,3}$), the precision is within one degree. A diagram of the UCF measurement setup can be found in the Supporting Information, Figure S3. The transmission spectra of the RE-doped polymer RWG sample were measured by the same spectrometer with a halogen white light source at different incident angles.

ASSOCIATED CONTENT

Supporting Information

SEM image, angle-resolved transmission spectra, and UCF measurement setup are given in the Supporting Information. This material is available free of charge via the Internet at http://pubs.acs.org.

AUTHOR INFORMATION

Corresponding Authors

*E-mail: phyhck@ccu.edu.tw.
*E-mail: phycch@ccu.edu.tw.

Notes

The authors declare no competing financial interest.

ACKNOWLEDGMENTS

The authors gratefully acknowledge financial support from the National Science Council (now called Ministry of Science and Technology), Taiwan, under grant Nos. NSC 101-2112-M-194-009-MY3, NSC 102-2112-M-194-004, MOST 103-221-E194-026, and 104-3113-E-008-004. J.H.L. acknowledges the support of a postdoctoral fellowship from National Science Council, Taiwan.

REFERENCES

(1) Ostrowski, A. D.; Chan, E. M.; Gargas, D. J.; Katz, E. M.; Han, G.; Schuck, P. J.; Milliron, D. J.; Cohen, B. E. Controlled Synthesis and Single-Particle Imaging of Bright, Sub-10 nm Lanthanide-Doped Upconverting Nanocrystals. *ACS Nano* **2012**, *6*, 2686−2692.

DOI: 10.1021/ph500427k
ACS Photonics 2015, 2, 530−536

(2) Auzel, F. Upconversion and Anti-Stokes Processes with f and d Ions in Solids. *Chem. Rev.* **2004**, *104*, 139−173.
(3) Haase, M.; Schäfer, H. Upconverting Nanoparticles. *Angew. Chem., Int. Ed.* **2011**, *50*, 5808−5829.
(4) Hao, S.; Chen, G.; Yang, C. Sensing Using Rare-Earth-Doped Upconversion Nano-Particles. *Theranostics* **2013**, *3*, 331−345.
(5) Cui, S.; Yin, D.; Chen, Y.; Di, Y.; Chen, H.; Ma, Y.; Achilefu, S.; Gu, Y. In Vivo Targeted Deep-Tissue Photodynamic Therapy Based on Near-Infrared Light Triggered Upconversion Nanoconstruct. *ACS Nano* **2013**, *7*, 676−688.
(6) Wang, Y. F.; Liu, G. Y.; Sun, L. D.; Xiao, J. W.; Zhou, J. C.; Yan, C. H. Nd^{3+}-Sensitized Upconversion Nanophosphors: Efficient in Vivo Bioimaging Probes with Minimized Heating Effect. *ACS Nano* **2013**, *7*, 7200−7206.
(7) Sanders, S.; Waarts, R. G.; Mehuys, D. G.; Wetch, D. F. Laser Diode Pumped 106 mW Blue Upconversion Fiber Laser. *Appl. Phys. Lett.* **1995**, *67*, 1815−1817.
(8) Downing, E.; Hesselink, L.; Ralston, J.; Macfarlane, R. A Three-Color, Solid-State, Three-Dimensional Display. *Science* **1996**, *273*, 1185−1189.
(9) Shalav, A.; Richards, B. S.; Trupke, T.; Krämer, K. W.; Güdel, H. U. Application of $NaYF_4:Er^{3+}$ Up-Converting Phosphors for Enhanced Near-Infrared Silicon Solar Cell Response. *Appl. Phys. Lett.* **2005**, *86*, 013505(1−3).
(10) DaCosta, M. V.; Doughan, S.; Han, Y.; Krull, U. J. Lanthanide Upconversion Nanoparticles and Applications in Bioassays and Bioimaging: A Review. *Anal. Chim. Acta* **2014**, *832*, 1−33.
(11) Yang, L. W.; Han, H. L.; Zhang, Y. Y.; Zhong, J. X. White Emission by Frequency Up-Conversion in Yb^{3+}-Ho^{3+}-Tm^{3+} Triply Doped Hexagonal $NaYF_4$ Nanorods. *J. Phys. Chem. C* **2009**, *113*, 18995−18999.
(12) Heer, S.; Kömpe, K.; Güdel, H. U.; Haase, M. Highly Efficient Multicolour Upconversion Emission in Transparent Colloids of Lanthanide-Doped $NaYF_4$ Nanocrystals. *Adv. Mater.* **2004**, *16*, 2102−2105.
(13) Schietinger, S.; Aichele, T.; Wang, H.-Q.; Nann, T.; Benson, O. Plasmon-Enhanced Upconversion in Single $NaYF_4:Yb^{3+}/Er^{3+}$ Codoped Nanocrystals. *Nano Lett.* **2010**, *10*, 134−138.
(14) Zhang, W.; Ding, F.; Chou, S. Y. Large Enhancement of Upconversion Luminescence of $NaYF_4/Yb^{3+}/Er^{3+}$ Nanocrystal by 3D Plasmonic Nano-Antennas. *Adv. Mater.* **2012**, *24*, OP236−OP241.
(15) Luu, Q.; Hor, A.; Fisher, J.; Anderson, R. B.; Liu, S.; Luk, T.-S.; Paude, H. P.; Baroughi, M. F.; May, P. S.; Smith, S. Two-Color Surface Plasmon Polariton Enhanced Upconversion in $NaYF_4$:Yb:Tm Nanoparticles on Au Nanopillar Arrays. *J. Phys. Chem. C* **2014**, *118*, 3251−3257.
(16) Wang, S. S.; Magnusson, R. Theory and Applications of Guided-Mode Resonance Filters. *Appl. Opt.* **1993**, *32*, 2606−2613.
(17) Soria, S.; Thayil K. N, A.; Badenes, G.; Bader, M. A.; Selle, A.; Marowsky, G. Resonant Double Grating Waveguide Structures As Enhancement Platforms for Two-Photon Fluorescence Excitation. *Appl. Phys. Lett.* **2005**, *87*, 081109(1−3).
(18) Ganesh, N.; Cunningham, B. T. Photonic-Crystal Near-Ultraviolet Reflectance Filters Fabricated by Nanoreplica Molding. *Appl. Phys. Lett.* **2006**, *88*, 071110(1−3).
(19) Ganesh, N.; Zhang, W.; Mathias, P. C.; Chow, E.; Soares, J. A. N. T.; Malyarchuk, V.; Smith, A. D.; Cunningham, B. T. Enhanced Fluorescence Emission from Quantum Dots on a Photonic Crystal Surface. *Nat. Nanotechnol.* **2007**, *2*, 515−520.
(20) Pokhriyal, A.; Lu, M.; Chaudhery, V.; Huang, C.-S.; Schulz, S.; Cunningham, B. T. Photonic Crystal Enhanced Fluorescence Using a Quartz Substrate to Reduce Limits of Detection. *Opt. Express* **2010**, *18*, 24793−24808.
(21) Siltanen, M.; Leivo, S.; Voima, P.; Kauranen, M.; Karvinen, P.; Vahimaa, P.; Kuittinen, M. Strong Enhancement of Second-Harmonic Generation in All-Dielectric Resonant Waveguide Grating. *Appl. Phys. Lett.* **2007**, *91*, 111109(1−3).
(22) Saari, A.; Genty, G.; Siltanen, M.; Karvinen, P.; Vahimaa, P.; Kuittinen, M.; Kauranen, M. Giant Enhancement of Second-Harmonic Generation in Multiple Diffraction Orders from Sub-Wavelength Resonant Waveguide Grating. *Opt. Express* **2010**, *18*, 12298−12303.
(23) Lin, J. H.; Tseng, C.-Y.; Lee, C.-T.; Young, J. F.; Kan, H.-C.; Hsu. Strong Guided Mode Resonant Local Field Enhanced Visible Harmonic Generation in an Azo-Polymer Resonant Waveguide Grating. C. C. *Opt. Express* **2014**, *22*, 2790−2797.
(24) Lin, J. H.; Tseng, C.-Y.; Lee, C.-T.; Kan, H.-C.; Hsu, C. C. Guided-Mode Resonance Enhanced Excitation and Extraction of Two-Photon Photoluminescence in a Resonant Waveguide Grating. *Opt. Express* **2013**, *21*, 24318−24325.
(25) Moharam, M. G.; Gaylord, T. K. Rigorous Coupled-Wave Analysis of Planar-Grating Diffraction. *J. Opt. Soc. Am.* **1981**, *71*, 811−818.
(26) Lai, N. D.; Liang, W. P.; Lin, J. H.; Hsu, C. C. Rapid Fabrication of Large-Area Periodic Structures Containing Well-Defined Defects by Combining Holography and Mask Techniques. *Opt. Express* **2005**, *13*, 5331−5337.
(27) Lai, N. D.; Liang, W. P.; Lin, J. H.; Hsu, C. C.; Lin, C. H. Fabrication of Two- and Three-Dimensional Periodic Structures by Multi-Exposure of Two-Beam Interference Technique. *Opt. Express* **2005**, *13*, 9605−9611.
(28) Http://refractiveindex.info/legacy/?group=GLASSES&material=BK7.
(29) Zhao, J.; Jin, D.; Schartner, E. P.; Lu, Y.; Liu, Y.; Zvyagin, A. V.; Zhang, L.; Dawes, J. M.; Xi, P.; Piper, J. A.; Goldys, E. M.; Monro, T. M. Single-Nanocrystal Sensitivity Achieved by Enhanced Upconversion Luminescence. *Nat. Nanotechnol.* **2013**, *8*, 729−734.
(30) Pollnau, M.; Gamelin, D. R.; Lüthi, S. R.; Güdel, H. U.; Hehlen, M. P. Power Dependence of Upconversion Luminescence in Lanthanide and Transition-Metal-Ion Systems. *Phys. Rev. B* **2000**, *61*, 3337−3346.
(31) Suyver, J. F.; Aebischer, A.; Garcia-Revilla, S.; Gerner, P.; Güdel, H. U. Anomalous Power Dependence of Sensitized Upconversion Luminescence. *Phys. Rev. B* **2005**, *71*, 125123-1−125123-9.
(32) Wei, Y.; Lu, F.; Zhang, X.; Chen, D. Synthesis and Characterization of Efficient Near-Infrared Upconversion Yb and Tm Codoped $NaYF_4$ Nanocrystal Reporter. *J. Alloys Compd.* **2007**, *427*, 333−340.
(33) Wang, G.; Qin, W.; Wang, L.; Wei, G.; Zhu, P.; Kim, R. Intense Ultraviolet Upconversion Lminescence from Hexagonal $NaYF_4:Yb^{3+}/Tm^{3+}$ Microcrystals. *Opt. Express* **2008**, *16*, 11907−11914.
(34) Qiu, H.; Yang, C.; Shao, W.; Damasco, J.; Wang, X.; Agren, H.; Prasad, P. N.; Chen, G. Enhanced Upconversion Luminescence in Yb^{3+}/Tm^{3+}-Codoped Fluoride Active Core/Active Shell/Inert Shell Nanoparticles through Directed Energy Migration. *Nanomaterials* **2014**, *4*, 55−68.
(35) Cao, B. S.; Wu, J. L.; Feng, Z. Q.; Dong, B. Investigation of Near-Infrared-to-Ultraviolet Upconversion Luminescence of Tm^{3+} Doped $NaYF_4$ Phosphors by Yb^{3+} Codoping. *Mater. Chem. Phys.* **2013**, *142*, 333−338.
(36) Zhang, Y. Y.; Yang, L. W.; Han, H. L.; Zong, J. X. Excitation Power Controlled Luminescence Switching in Yb^{3+}-Tm^{3+} Co-Doped Hexagonal $NaYF_4$ Nanorods. *Opt. Commun.* **2009**, *282*, 2857−2860.
(37) Yi, G. S.; Chow, G. M. Synthesis of Hexagonal-Phase $NaYF_4$:Yb,Er and $NaYF_4$:Yb,Tm Nanocrystals with Efficient Up-Conversion Fluorescence. *Adv. Funct. Mater.* **2006**, *16*, 2324−2329.

DOI: 10.1021/ph500427k
ACS Photonics 2015, 2, 530−536